Article

TRANSACTIONS OF THE INSTITUTE OF MEASUREMENT & CONTROL

Transactions of the Institute of Measurement and Control
1–11

DOI: 10.1177/0142331217737362
journals.sagepub.com/home/tim
SAGE

Design of a decoupling strategy and parameter calculation for six-phase PM machines with general angular displacement

Guillermo Catuogno[1], Gaston Frias[1], Guillermo Garcia[2] and Roberto Leidhold[3]

Abstract

A novel decoupling model for a six-phase permanent magnet machine is proposed in this paper. The model considers the machine as two independent three-phase stator windings that are spatially shifted by a generic angle α. The proposed transformation considers the zero sequence and allows the coupling between phases to be eliminated. The parameters, which define the dynamic behaviour of the model, are calculated with simulations performed using the finite-element method. The decoupled model and the parameters are analyzed for two configurations of a traditional six-phase machine. Simulation results were validated by experimental results with a simple procedure.

Keywords

Six-phase permanent magnet machine, decoupling model, parameter calculation

Introduction

In general, polyphase machines show better fault tolerance and size reduction per phase of the converter than conventional three-phase machines (Levi et al., 2016).

Among polyphase machines, the use of six-phase polyphase machines has increased recently, owing to their advantage of having a number of phases that is a multiple of three, which allows the use of well-known available technologies, such as three-phase power converters, signal adapters and control strategies. There are different configurations for six-phase machines, depending on the angular displacement (α) between each three-phase stator winding. For many years, asymmetric machines ($\alpha = 30°$) have been a better option, compared with symmetric ones ($\alpha = 60°$) (Barrero and Duran, 2016; Levi, 2008). This is mainly because of the advantage they show regarding the cancellation of harmonics in torque pulsations using six-pulse inverters. However, owing to advances in power electronics, their high switching frequency and pulse-width modulation strategies, they allow for both configurations presented in Figure 1 to have similar performances in relation to torque pulsations (Munim et al., 2016).

With regard to the analytical modelling of a six-phase machine, the following models stand out among many proposals:

- Vector space decomposition;
- Double three-phase.

The first model, based on the decomposition of the vector space for six-phase polyphase machines, commonly known as vector space decomposition, presented in Zhao and Lipo (1995), is the most widespread (Bojoi et al., 2003). It allows the voltage and currents of the machine to be represented in three pairs of windings. Each orthogonal sub-space is commonly represented as $\alpha_1\beta_2$, x_1x_2 and 0_10_2.

The first sub-space, $\alpha_1\beta_2$, contains the fundamental and the harmonics $12n\pm1$, with $(n = 1, 2, 3, \ldots)$. This sub-space is in charge of producing the machine electromagnetic torque. The second sub-space, x_1x_2, contains the harmonics $6n\pm1$ for $(n = 1, 3, 5, \ldots)$. Unlike sub-space $\alpha_1\beta_2$, it does not produce torque. Finally, the 0_10_2 plane maps the zero-sequence components of the machine, which are not taken into account when the neutral is not connected.

Numerous works based on the vector space decomposition model have been proposed in the literature, aiming at minimizing torque pulsations. Karttunen et al. (2014), besides the torque control performed on the sub-plane $\alpha_1\beta_2$, use the remaining degree of freedom to control the sub-plane x_1x_2 in

[1]Automatic Control Laboratory, Faculty of Engineering and Agricultural Sciences, National University of San Luis, Argentina
[2]Applied Electronics Group, Faculty of Engineering, National University of Río Cuarto, Argentina
[3]Institute of Electrical Energy Systems, Otto von Guericke University, Germany

Corresponding author:
Guillermo Catuogno, Automatic Control Laboratory (LCA), National University of San Luis (UNSL), V. Mercedes, San Luis, Argentina.
Email: grcatu@gmail.com

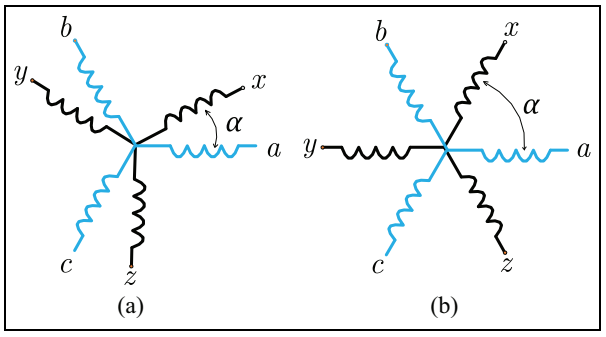

Figure 1. Configurations: a) asymmetric, b) symmetric.

order to minimize the harmonic components produced by EMF imbalances and harmonics. The same principle is applied by Che et al. (2014), but in this case the sub-plane x_1x_2 is used to compensate the harmonics due to the inverter dead-times.

The second model involves considering the machine as two independent three-phase windings (double three-phase). The result is two systems, $\alpha_1\beta_1 0_1$ and $\alpha_2\beta_2 0_2$, on which conventional control strategies for three-phase machines can be applied (Nelson and Krause, 1974).

Although it seems, at first sight, that the double three-phase model is simpler, it is demonstrated in Karttunen et al. (2012) that considering the machine as two three-phase windings causes complex couplings between them, which are difficult to compensate.

Also, Schiferl and Ong (1983) analyzed a six-phase polyphase machine with an arbitrary displacement angle, based on Parks transformation. However, this model is not represented in decoupled *d-q* reference frames either; thereby, a further transformation is needed to decouple the two *d-q* reference frames from each other.

Variants of the double three-phase model that allow elimination of coupling between both three-phase systems and for an arbitrary angle are proposed by Andriollo et al. (2009), Camillis et al. (2001) and Kallio et al. (2013). However, for this variation, the zero sequence as well as its coupling are not taken into account.

Once the new model is defined, it is important to determine the fundamental parameters, stator resistance and winding inductance, of the electric machine accurately, as they determine the dynamic behaviour of the machine.

The more precise the parameters of the machine, the better the behaviour of the control strategies based on the model will be, as they can affect the machine performance. In addition, these parameters are important to predict system behaviour during a failure situation.

There are different methods to measure inductance in electric machines. Broadly, they can be classified as offline (Dutta and Rahman, 2006) and online (Underwood and Husain, 2010) methods. Online methods are very effective, since the inductances vary with different operating conditions. However, the online measurements often lead to numerical algorithms, such as the recursive least-square method (Underwood and Husain, 2010).

From the previous considerations, in this work we propose a novel double three-phase model that defines a new transformation Q, which allows the coupling between phases to be eliminated. The transformation is applied on two traditional configurations of six-phase polyphase machines, the asymmetric and symmetric setups. In addition, this variation of the double three-phase model includes the zero sequence, which may be significantly useful in fault-tolerant systems (Catuogno et al., 2016). Once the model is defined, the machine parameters are calculated by finite-element simulation and validated with an experimental offline method developed for three-phase machines that is much easier to apply.

Machine model

The six-phase polyphase machine model in phase variables *abcxyz*, can be represented by

$$\vec{v}_{abcxyz} = \mathbf{R_s}\vec{i}_{abcxyz} + \mathbf{L_s}\frac{\mathrm{d}}{\mathrm{d}t}\vec{i}_{abcxyz} + \vec{e}_{abcxyz} \tag{1}$$

where $\vec{v}_{abcxyz}$, $\vec{i}_{abcxyz}$ and $\vec{e}_{abcxyz}$ are the vectors that represent the voltage, current and EMF of the phases *abcxyz*. The latter can be defined as

$$e_j = \frac{\mathrm{d}\psi_j}{\mathrm{d}t} = \frac{\mathrm{d}\psi_j}{\mathrm{d}\theta}\frac{\mathrm{d}\theta}{\mathrm{d}t} = \varphi_j(\theta)\omega \tag{2}$$

with $j = a, b, c, x, y, z$, where ψ_j are the fluxes linked by the stator, $\mathrm{d}\theta/\mathrm{d}t = \omega$ is the rotor angular speed and $\varphi_j(\theta)$ is a function that depends on the flux density distribution in the air gap and also determines the waveform of the induced EMF. These functions depend on the geometrical configuration of the stator windings, as well as on the shape and location of the magnets and the stator core. $\mathbf{R_s}$ and $\mathbf{L_s}$ are the resistance and inductance matrix of the stator windings, respectively

$$\mathbf{R_s} = \begin{bmatrix} 0 & r_\mathrm{s} & 0 & 0 & 0 & 0 \\ 0 & 0 & r_\mathrm{s} & 0 & 0 & 0 \\ 0 & 0 & 0 & r_\mathrm{s} & 0 & 0 \\ 0 & 0 & 0 & 0 & r_\mathrm{s} & 0 \\ 0 & 0 & 0 & 0 & 0 & r_\mathrm{s} \end{bmatrix} \tag{3}$$

and

$$\mathbf{L_s} = \begin{bmatrix} L_\mathrm{s} & M_\mathrm{s} & M_\mathrm{s} & M_1 & M_2 & M_3 \\ M_\mathrm{s} & L_\mathrm{s} & M_\mathrm{s} & M_3 & M_1 & M_2 \\ M_\mathrm{s} & M_\mathrm{s} & L_\mathrm{s} & M_2 & M_3 & M_1 \\ M_1 & M_3 & M_2 & L_\mathrm{s} & M_\mathrm{s} & M_\mathrm{s} \\ M_2 & M_1 & M_3 & M_\mathrm{s} & L_\mathrm{s} & M_\mathrm{s} \\ M_3 & M_2 & M_1 & M_\mathrm{s} & M_\mathrm{s} & L_\mathrm{s} \end{bmatrix} \tag{4}$$

The following considerations were made regarding the inductance matrix $\mathbf{L_s}$

$$\begin{aligned} L_\mathrm{s} &= L_{aa} = L_{bb} = L_{cc} = L_{xx} = L_{yy} = L_{zz} \\ M_\mathrm{s} &= M_{ab} = M_{bc} = M_{ca} = M_{xy} = M_{xz} = M_{zy} \\ M_1 &= M_{ax} = M_{by} = M_{cz} \\ M_2 &= M_{ay} = M_{bz} = M_{cx} \\ M_3 &= M_{az} = M_{bx} = M_{cy} \end{aligned} \tag{5}$$

The inductances defined in equation (5) can also be represented as a function of the phase angle α between the two three-phase systems *abc* and *xyz*, as

$$\begin{aligned} M_s &= M\cos(2\pi/3) \\ M_1 &= M\cos(\alpha) \\ M_2 &= M\cos(2\pi/3+\alpha) \\ M_3 &= M\cos(4\pi/3+\alpha) \end{aligned} \tag{6}$$

where M is the mutual inductance of two phases if they are aligned.

The model proposed in this paper consists of a double three-phase system. That is, the modelling of two three-phase systems independently, including, in this case, the neutral connection. With the objective of simplifying the equations for the model proposed in equations (1) and (2), the following transformation was carried out first

$$\vec{f}_{\alpha_1\beta_1 0_1 \alpha_2\beta_2 0_2} = \mathbf{K_1}.\vec{f}_{abcxyz} \tag{7}$$

where $\mathbf{K_1}$ is a 6×6 matrix defined as

$$\mathbf{K_1} = \begin{bmatrix} \mathbf{K} & 0 \\ 0 & \mathbf{K} \end{bmatrix} \tag{8}$$

where $\mathbf{K}$ is the power invariant Clarke Transformation defined as

$$\mathbf{K} = \sqrt{\frac{2}{3}}\begin{bmatrix} 1 & \frac{-1}{2} & \frac{-1}{2} \\ 0 & \frac{\sqrt{3}}{2} & \frac{-\sqrt{3}}{2} \\ \frac{1}{\sqrt{2}} & \frac{1}{\sqrt{2}} & \frac{1}{\sqrt{2}} \end{bmatrix} \tag{9}$$

where $\vec{f}$ is a generic vector that can represent current, voltage, flux or the EMF of the stator.

Using the Clarke transformation, the following six-phase polyphase machine model in variables $\alpha_1\beta_1 0_1$ and $\alpha_2\beta_2 0_2$ can be obtained

$$\begin{aligned} \vec{v}_{\alpha_1\beta_1 0_1 \alpha_2\beta_2 0_2} &= \mathbf{R}\vec{i}_{\alpha_1\beta_1 0_1 \alpha_2\beta_2 0_2} \\ &+ \mathbf{L}\frac{\mathrm{d}}{\mathrm{d}t}\vec{i}_{\alpha_1\beta_1 0_1 \alpha_2\beta_2 0_2} + \vec{e}_{\alpha_1\beta_1 0_1 \alpha_2\beta_2 0_2} \end{aligned} \tag{10}$$

where $\vec{v}_{\alpha_1\beta_1 0_1 \alpha_2\beta_2 0_2}$, $\vec{i}_{\alpha_1\beta_1 0_1 \alpha_2\beta_2 0_2}$, and $\vec{e}_{\alpha_1\beta_1 0_1 \alpha_2\beta_2 0_2}$ represent the voltage, current and EMF of the stator and $\mathbf{R}$ and $\mathbf{L}$ are stator winding resistance and inductance matrices.

Such matrices are obtained as

$$\begin{aligned} \mathbf{R} &= \mathbf{K_1}\cdot\mathbf{R_s}\cdot\mathbf{K_1^{-1}} \\ \mathbf{L} &= \mathbf{K_1}\cdot\mathbf{L_s}\cdot\mathbf{K_1^{-1}} \end{aligned} \tag{11}$$

resulting in

$$\mathbf{R} = \begin{bmatrix} r_s & 0 & 0 & 0 & 0 & 0 \\ 0 & r_s & 0 & 0 & 0 & 0 \\ 0 & 0 & r_s & 0 & 0 & 0 \\ 0 & 0 & 0 & r_s & 0 & 0 \\ 0 & 0 & 0 & 0 & r_s & 0 \\ 0 & 0 & 0 & 0 & 0 & r_s \end{bmatrix} \tag{12}$$

and

$$\mathbf{L} = \begin{bmatrix} L_s^* & 0 & 0 & M_b & M_a & 0 \\ 0 & L_s^* & 0 & -M_a & M_b & 0 \\ 0 & 0 & L_0^* & 0 & 0 & M_c \\ M_b & -M_a & 0 & L_s^* & 0 & 0 \\ M_a & M_b & 0 & 0 & L_s^* & 0 \\ 0 & 0 & M_c & 0 & 0 & L_0^* \end{bmatrix} \tag{13}$$

where

$$\begin{aligned} L_s^* &= L_s - M_s \\ L_0^* &= L_s + 2M_s \\ M_a &= \frac{\sqrt{3}}{2}M_3 - \frac{\sqrt{3}}{2}M_2 \\ M_b &= M_1 - \frac{1}{2}M_2 - \frac{1}{2}M_3 \\ M_c &= M_1 + M_2 + M_3 \end{aligned} \tag{14}$$

Different inductance couplings between both of the three phase windings systems can be observed in equation (13). Owing to this coupling, the two three-phase windings are not independent. This leads to a more complex control strategy or, in the case of non-consideration, affects the performance of the system. Therefore, in this paper it is proposed that the couplings are evaluated and eliminated to simplify the control design.

To do this, a diagonalization of equation (13) is proposed, with the aim of finding a transformation $\mathbf{P}$ that allows a diagonal matrix $\mathbf{L_D}$ to be obtained that fulfils

$$\mathbf{L_D} = \mathbf{P}^{-1}\cdot\mathbf{L}\cdot\mathbf{P} \tag{15}$$

The transformation matrix $\mathbf{P}$ can be built by arranging, column by column, the eigenvectors of $\mathbf{L}$ (Robbiano, 2011); hence, the elements of $\mathbf{L_D}$ will result in the eigenvalues of $\mathbf{L}$. A tool for symbolic computation was used to obtain the eigenvectors and eigenvalues, yielding

$$\mathbf{P} = \begin{bmatrix} \frac{M_b}{M_x} & \frac{M_a}{M_x} & 0 & -\frac{M_b}{M_x} & -\frac{M_a}{M_x} & 0 \\ -\frac{M_a}{M_x} & \frac{M_b}{M_x} & 0 & \frac{M_a}{M_x} & -\frac{M_b}{M_x} & 0 \\ 0 & 0 & 1 & 0 & 0 & -1 \\ 1 & 0 & 0 & 1 & 0 & 0 \\ 0 & 1 & 0 & 0 & 1 & 0 \\ 0 & 0 & 1 & 0 & 0 & 1 \end{bmatrix} \tag{16}$$

where

$$M_x = \sqrt{M_a^2 + M_b^2} \tag{17}$$

$$\mathbf{L_D} = \begin{bmatrix} L_{d1} & 0 & 0 & 0 & 0 & 0 \\ 0 & L_{d2} & 0 & 0 & 0 & 0 \\ 0 & 0 & L_{d3} & 0 & 0 & 0 \\ 0 & 0 & 0 & L_{d4} & 0 & 0 \\ 0 & 0 & 0 & 0 & L_{d5} & 0 \\ 0 & 0 & 0 & 0 & 0 & L_{d6} \end{bmatrix} \tag{18}$$

with

$$\begin{aligned} L_{d1} &= L_{d2} = L_s - M_s + M_x \\ L_{d3} &= L_s + 2M_s + M_c \\ L_{d4} &= L_{d5} = L_s - M_s - M_x \\ L_{d6} &= L_s + 2M_s - M_c \end{aligned} \tag{19}$$

From equation (16), it can be observed that the inductance matrix depends on a component that contains values L_s and M_s from one of the three-phase windings and also mutual inductances from the remaining three-phase winding formed by M_1, M_2 and M_3. Inductances M_1, M_2 and M_3 are different, depending on the phase angle between two three-phase windings. By substituting equation (6) into the matrix $\mathbf{P}$ obtained in equation (16), it is possible to obtain the transformation matrix that depends only on the phase angle α

$$\mathbf{P} = \begin{bmatrix} -\cos(\alpha) & \sin(\alpha) & 0 & \cos(\alpha) & -\sin(\alpha) & 0 \\ -\sin(\alpha) & -\cos(\alpha) & 0 & \sin(\alpha) & \cos(\alpha) & 0 \\ 0 & 0 & 1 & 0 & 0 & -1 \\ 1 & 0 & 0 & 1 & 0 & 0 \\ 0 & 1 & 0 & 0 & 1 & 0 \\ 0 & 0 & 1 & 0 & 0 & 1 \end{bmatrix} \tag{20}$$

and its inverse transformation $\mathbf{P^{-1}}$

$$\mathbf{P^{-1}} = \begin{bmatrix} \frac{-\cos(\alpha)}{2} & \frac{-\sin(\alpha)}{2} & 0 & \frac{1}{2} & 0 & 0 \\ \frac{\sin(\alpha)}{2} & \frac{-\cos(\alpha)}{2} & 0 & 0 & \frac{1}{2} & 0 \\ 0 & 0 & \frac{1}{2} & 0 & 0 & \frac{1}{2} \\ \frac{\cos(\alpha)}{2} & \frac{\sin(\alpha)}{2} & 0 & \frac{1}{2} & 0 & 0 \\ \frac{-\sin(\alpha)}{2} & \frac{\cos(\alpha)}{2} & 0 & 0 & \frac{1}{2} & 0 \\ 0 & 0 & -\frac{1}{2} & 0 & 0 & \frac{1}{2} \end{bmatrix} \tag{21}$$

Finally, the model of the machine in the new coordinate system will be obtained from the transformations

$$\vec{f}_{p_1p_2p_3p_4p_5p_6} = \mathbf{Q}\,\vec{f}_{abcxyz} \tag{22}$$

where

$$\mathbf{Q} = \sqrt{2} \cdot \mathbf{P}^{-1} \cdot \mathbf{K_1} \tag{23}$$

where the term $\sqrt{2}$ is included to ensure that the transformation $\mathbf{Q}$ is power invariant and this new transformation allows the model proposed in equation (1) to be obtained in the new coordinate system $p_1p_2p_3p_4p_5p_6$, as

$$\vec{v}_{p_1p_2p_3p_4p_5p_6} = \mathbf{R_s}\vec{i}_{p_1p_2p_3p_4p_5p_6} + \mathbf{L_D}\frac{\mathrm{d}}{\mathrm{d}t}\vec{i}_{p_1p_2p_3p_4p_5p_6} + \vec{e}_{p_1p_2p_3p_4p_5p_6} \tag{24}$$

where the transformation $\mathbf{Q}$ is responsible for the elimination of the coupling effects in equations (4) and (13) and can take different values, depending on the phase angle α between the two three-phase windings in equation (25)

$$\mathbf{Q} = \sqrt{3}\begin{bmatrix} \frac{-\cos(\alpha)}{3} & \frac{-\cos(\alpha-23\pi)}{3} & \frac{-\cos(\alpha-43\pi)}{3} & \frac{1}{3} & -\frac{1}{6} & -\frac{1}{6} \\ \frac{\sin(\theta)}{3} & \frac{\sin(\alpha-23\pi)}{3} & \frac{\sin(\alpha-43\pi)}{3} & 0 & \frac{\sqrt{3}}{6} & -\frac{\sqrt{3}}{6} \\ \frac{\sqrt{2}}{6} & \frac{\sqrt{2}}{6} & \frac{\sqrt{2}}{6} & \frac{\sqrt{2}}{6} & \frac{\sqrt{2}}{6} & \frac{\sqrt{2}}{6} \\ \frac{\cos(\theta)}{3} & \frac{\cos(\alpha-23\pi)}{3} & \frac{\cos(\alpha-43\pi)}{3} & \frac{1}{3} & -\frac{1}{6} & -\frac{1}{6} \\ \frac{-\sin(\theta)}{3} & \frac{-\sin(\alpha-23\pi)}{3} & \frac{-\sin(\alpha-43\pi)}{3} & 0 & \frac{\sqrt{3}}{6} & -\frac{\sqrt{3}}{6} \\ -\frac{\sqrt{2}}{6} & -\frac{\sqrt{2}}{6} & -\frac{\sqrt{2}}{6} & \frac{\sqrt{2}}{6} & \frac{\sqrt{2}}{6} & \frac{\sqrt{2}}{6} \end{bmatrix} \tag{25}$$

From the new transformation $\mathbf{Q}$ found in equation (25), the power equation can be written as a function of the new coordinate system $p_1p_2p_3p_4p_5p_6$ as

$$p = \left(\mathbf{Q^{-1}}.\mathbf{i}_{p_1p_2p_3p_4p_5p_6}\right)^{\mathrm{T}}.\mathbf{Q}^{-1}.\mathbf{v}_{p_1p_2p_3p_4p_5p_6} \tag{26}$$

By considering, the transformation defined in (25), the following term yields the identity matrix

$$\left(\mathbf{Q^{-1}}\right)^{\mathrm{T}}.\mathbf{Q^{-1}} = \mathbf{I_{6\times 6}} \tag{27}$$

and therefore the power is

$$p = i_{p_1}v_{p_1} + i_{p_2}v_{p_2} + i_{p_3}v_{p_3} + i_{p_4}v_{p_4} + i_{p_5}v_{p_5} + i_{p_6}v_{p_6} \tag{28}$$

which demonstrates, that the transformation is power invariant. The developed methodology simplifies the analysis of the six-phase polyphase machine generator by converting the six-phase equations described in equation (1) into two decoupled three-phase systems.

Study cases

In this section, we analyze the configurations presented in Figure 1, to find the matrix $\mathbf{Q}$ that allows the diagonal matrix to be obtained for each of them. In subsequent sections, the parameters for these configurations will be obtained.

Asymmetric machine

This is perhaps the most widespread configuration within six-phase machines; its angle α is

$$\alpha = 30^\circ \tag{29}$$

Substituting equation (29) into equations (20) and (21), the transformation matrices $\mathbf{P}$ and $\mathbf{P^{-1}}$ are obtained

$$\mathbf{P} = \begin{bmatrix} -\frac{\sqrt{3}}{2} & \frac{1}{2} & 0 & \frac{\sqrt{3}}{2} & -\frac{1}{2} & 0 \\ -\frac{1}{2} & -\frac{\sqrt{3}}{2} & 0 & \frac{1}{2} & \frac{\sqrt{3}}{2} & 0 \\ 0 & 0 & 1 & 0 & 0 & -1 \\ 1 & 0 & 0 & 1 & 0 & 0 \\ 0 & 1 & 0 & 0 & 1 & 0 \\ 0 & 0 & 1 & 0 & 0 & 1 \end{bmatrix} \tag{30}$$

$$\mathbf{P^{-1}} = \begin{bmatrix} -\frac{\sqrt{3}}{4} & -\frac{1}{4} & 0 & \frac{1}{2} & 0 & 0 \\ \frac{1}{4} & -\frac{\sqrt{3}}{4} & 0 & 0 & \frac{1}{2} & 0 \\ 0 & 0 & \frac{1}{2} & 0 & 0 & \frac{1}{2} \\ \frac{\sqrt{3}}{4} & 1/4 & 0 & \frac{1}{2} & 0 & 0 \\ -\frac{1}{4} & \frac{\sqrt{3}}{4} & 0 & 0 & \frac{1}{2} & 0 \\ 0 & 0 & -\frac{1}{2} & 0 & 0 & \frac{1}{2} \end{bmatrix} \quad (31)$$

and the new transformation matrix is $\mathbf{Q} = \sqrt{2} \cdot \mathbf{P^{-1}} \cdot \mathbf{K_1}$

$$\mathbf{Q} = \sqrt{3} \begin{bmatrix} -\frac{\sqrt{3}}{6} & 0 & \frac{\sqrt{3}}{6} & \frac{1}{3} & -\frac{1}{6} & -\frac{1}{6} \\ \frac{1}{6} & -\frac{1}{3} & \frac{1}{6} & 0 & \frac{\sqrt{3}}{6} & -\frac{\sqrt{3}}{6} \\ \frac{\sqrt{2}}{6} & \frac{\sqrt{2}}{6} & \frac{\sqrt{2}}{6} & \frac{\sqrt{2}}{6} & \frac{\sqrt{2}}{6} & \frac{\sqrt{2}}{6} \\ \frac{\sqrt{3}}{6} & 0 & -\frac{\sqrt{3}}{6} & \frac{1}{3} & -\frac{1}{6} & -\frac{1}{6} \\ -\frac{1}{6} & \frac{1}{3} & -\frac{1}{6} & 0 & \frac{\sqrt{3}}{6} & -\frac{\sqrt{3}}{6} \\ -\frac{\sqrt{2}}{6} & -\frac{\sqrt{2}}{6} & -\frac{\sqrt{2}}{6} & \frac{\sqrt{2}}{6} & \frac{\sqrt{2}}{6} & \frac{\sqrt{2}}{6} \end{bmatrix} \quad (32)$$

Symmetric machine

In this case, the symmetric configuration presents a phase angle α between three-phase windings equal to

$$\alpha = 60^\circ \quad (33)$$

Substituting equation (33) into equations (20) and (21), the transformation matrices $\mathbf{P}$ and $\mathbf{P}^{-1}$ are obtained

$$\mathbf{P} = \begin{bmatrix} -\frac{1}{2} & \frac{\sqrt{3}}{2} & 0 & \frac{1}{2} & -\frac{\sqrt{3}}{2} & 0 \\ -\frac{\sqrt{3}}{2} & -\frac{1}{2} & 0 & \frac{\sqrt{3}}{2} & \frac{1}{2} & 0 \\ 0 & 0 & 1 & 0 & 0 & -1 \\ 1 & 0 & 0 & 1 & 0 & 0 \\ 0 & 1 & 0 & 0 & 1 & 0 \\ 0 & 0 & 1 & 0 & 0 & 1 \end{bmatrix} \quad (34)$$

$$\mathbf{P^{-1}} = \begin{bmatrix} -\frac{1}{4} & -\frac{\sqrt{3}}{4} & 0 & \frac{1}{2} & 0 & 0 \\ \frac{\sqrt{3}}{4} & -\frac{1}{4} & 0 & 0 & \frac{1}{2} & 0 \\ 0 & 0 & \frac{1}{2} & 0 & 0 & \frac{1}{2} \\ \frac{1}{4} & \frac{\sqrt{3}}{4} & 0 & \frac{1}{2} & 0 & 0 \\ -\frac{\sqrt{3}}{4} & \frac{1}{4} & 0 & 0 & \frac{1}{2} & 0 \\ 0 & 0 & -\frac{1}{2} & 0 & 0 & \frac{1}{2} \end{bmatrix} \quad (35)$$

and the new transformation matrix is $\mathbf{Q} = \sqrt{2} \cdot \mathbf{P}^{-1} \cdot \mathbf{K_1}$

$$\mathbf{Q} = \sqrt{3} \begin{bmatrix} -\frac{1}{6} & -\frac{1}{6} & \frac{1}{3} & \frac{1}{3} & -\frac{1}{6} & -\frac{1}{6} \\ \frac{\sqrt{3}}{6} & -\frac{\sqrt{3}}{6} & 0 & 0 & \frac{\sqrt{3}}{6} & -\frac{\sqrt{3}}{6} \\ \frac{\sqrt{2}}{6} & \frac{\sqrt{2}}{6} & \frac{\sqrt{2}}{6} & \frac{\sqrt{2}}{6} & \frac{\sqrt{2}}{6} & \frac{\sqrt{2}}{6} \\ \frac{1}{6} & \frac{1}{6} & -\frac{1}{3} & \frac{1}{3} & -\frac{1}{6} & -\frac{1}{6} \\ -\frac{\sqrt{3}}{6} & \frac{\sqrt{3}}{6} & 0 & 0 & \frac{\sqrt{3}}{6} & -\frac{\sqrt{3}}{6} \\ -\frac{\sqrt{2}}{6} & -\frac{\sqrt{2}}{6} & -\frac{\sqrt{2}}{6} & \frac{\sqrt{2}}{6} & \frac{\sqrt{2}}{6} & \frac{\sqrt{2}}{6} \end{bmatrix} \quad (36)$$

Interpreting the new transformation matrix Q

The transformation matrix $\mathbf{Q}$ was defined in the previous sections in equation (25) and applied to two configurations of six-phase machines in equations (32) and (36). Besides eliminating couplings between phases, these transformations produce a new reference system $p_1p_2p_3p_4p_5p_6$, as can be seen in Figure 2.

To understand the effects of the transformation $\mathbf{Q}$ on the phase variables *abcxyz*, it was applied to the electromotive force of the machines considered in the previous sections. As the transformed variables resulting from the two configurations analyzed in this paper are identical, only those from the asymmetric configuration are presented next. The waveform shown in Figure 3 was built out of the measured electromotive force from the available asymmetric machine over one period. In this figure, the EMF in *abcxyz* coordinates is presented, where the two three-phase systems with a 30° phase angle between them can be clearly observed. Each three-phase system consists of three 120° out-of-phase components.

The second coordinate system, $\alpha_1\beta_1 0_1 \alpha_2\beta_2 0_2$, shown in Figure 4, which is obtained from applying the transformation matrix $\mathbf{K_1}$, is composed of two three-phase systems with a 30° phase angle between them, as in the previous system, except that in this particular case, each system presents two orthogonal components plus the zero-sequence component (Clarke transformation on each three-phase system).

Finally, when the transformation $\mathbf{P^{-1}}$ is applied, the coordinate system $p_1p_2p_3p_4p_5p_6$ is obtained, which is composed of two systems with a 90° phase angle between them. As with the coordinate system $\alpha_1\beta_1 0_1 \alpha_2\beta_2 0_2$, each system is composed of two orthogonal components plus the zero-sequence component (Figure 5).

Measurement of parameters

With a machine model now defined, the next step is to s the parameters for the model. These are obtained by using experimental tests and finite-element simulations as described next.

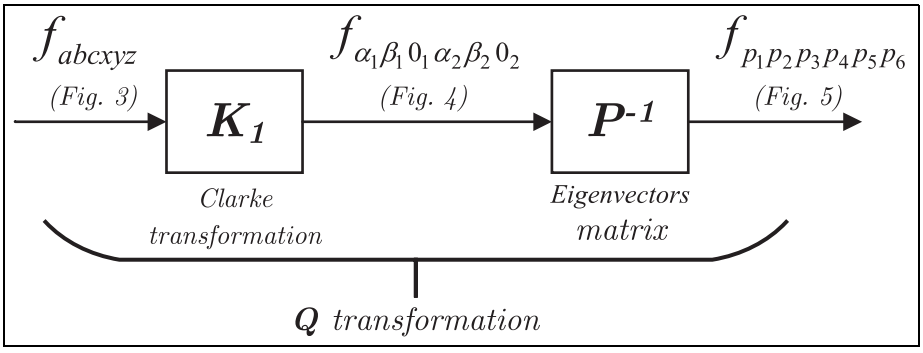

Figure 2. Transformation diagram.

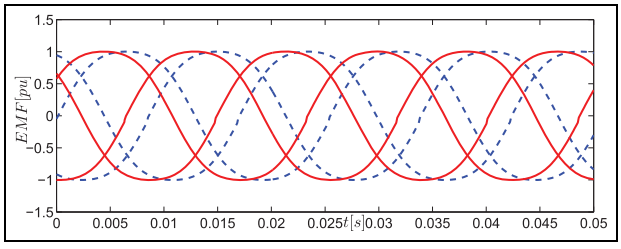

Figure 3. EMF in coordinates *abc* (solid lines) and *xyz* (dashed lines).

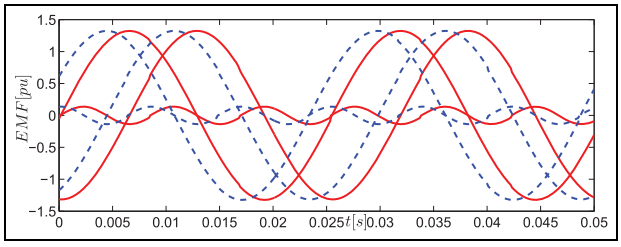

Figure 4. EMF in coordinates $\alpha_1\beta_1 0_1$ (solid lines) and $\alpha_2\beta_2 0_2$ (dashed lines).

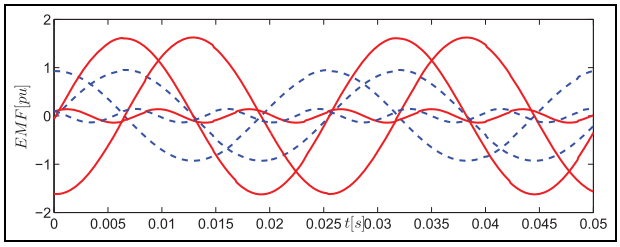

Figure 5. EMF in coordinates $p_1p_2p_3$ (solid lines) and $p_4p_5p_6$ (dashed lines).

Experimental tests

Regarding the *AC standstill method* proposed by Dutta and Rahman (2006) for three-phase machines, this involves measuring induced voltages for the different rotor positions or different current values.

Two six-phase polyphase machines are available in the laboratory, one of them presents an asymmetric configuration, and the other a symmetric configuration. The corresponding parameters are shown in Table 1. In Figure 6 the diagrams of the winding configurations of the two machines are presented.

The connection scheme for the test carried out on a six-phase star connected machine with accessible neutral is shown in Figure 7. One of the phase windings is excited by a single phase supply. The line current and the voltage induced in the remaining windings are measured for the proposed test. The self and mutual inductances can be estimated as

Table 1. SAsymmetric and symmetric machine parameters.

Parameter	Value	Parameter	Value
Phase shift (asymmetric)	30°	Magnets	Ferrite
Phase shift (symmetric)	60°	Winding	Series
Phases	6	Wire	AW18
Poles	4	Wires per coil	60
Slots	36	Wires per slot	120

$$L_{aa} = \frac{\sqrt{\left(\frac{V_a}{I_a}\right)^2 - R^2}}{(2\pi f)} \tag{37}$$

$$M_{ai} = \frac{V_i}{(2\pi f) I_a}, \quad \text{with} \quad i = b, c, x, y, z \tag{38}$$

where R is the stator resistance, V_a and f are the voltage and frequency of the power supply and I_a and V_{bcxyz} are the measured current and voltages, respectively.

In Figure 8 the experimental prototype is displayed.

Simulation test

Two magnetostatic 2D models of the six-phase machine were developed for the configurations analyzed in this work. Dimensions and material data from the experimental machines available in the laboratory were used for modelling in the software FEMM 4.2 (Meeker, 2009). The model developed in FEMM and the front view of the open experimental

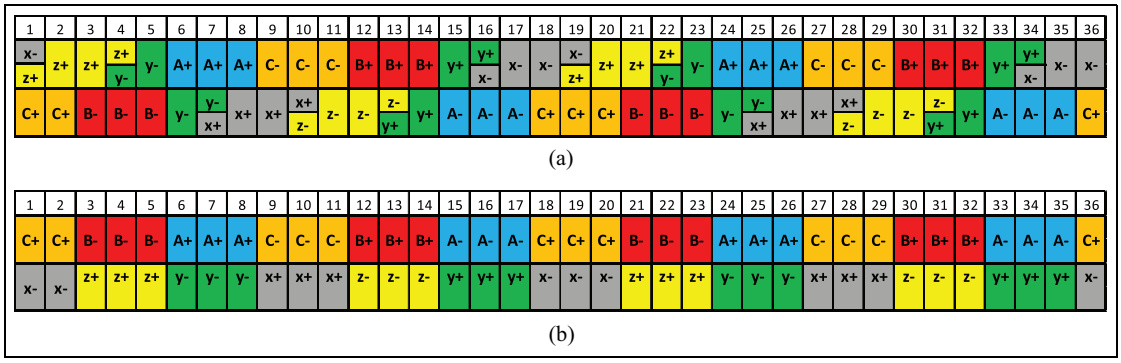

Figure 6. Winding configurations for (a) asymmetric and (b) symmetric machines.

machine are presented in Figure 9 for the case of the asymmetric configuration.

To calculate the inductance, different methods are available in the literature. According to Bianchi (2005), inductance can be obtained in three ways:

- Calculating L from magnetic energy;
- Calculating L from flux linkage;
- Calculating L from airgap flux density.

The second method was chosen for this work. First, the flux linkage was computed using the finite-element method; then the self and mutual inductances are calculated using the same procedure as for the experimental calculation, that is, by supplying current to the windings of one phase and then computing the flux linkage in the remaining windings. Then, only a single winding will carry current $i = I_a$, and the inductances can be calculated as (Bianchi, 2005)

$$L_{aa} = \frac{\psi_a(\theta)}{I_a} \tag{39}$$

$$M_{ai} = \frac{\psi_i(\theta)}{I_a}, \quad \text{with} \quad i = b, c, x, y, z \tag{40}$$

Results

Experimental

Two different tests were carried out for the asymmetric and symmetric machines. The first one, $E1$, involved measuring the inductance for a fixed current and different rotor positions. The second one, $E2$ involved measuring the inductance for a fixed rotor position and different values of current.

Figure 10 presents results of test $E1$ for the asymmetric machine. The inductances L_{aa} and M_{ai} calculated according to equations (37) and (38) are displayed as a function of the rotor position every 5°. It is possible to observe how inductance varies depending on position; this is due to the geometry and the characteristics of the machine.

Figure 11 presents the results of test $E2$ for a fixed rotor position ($\theta = 0°$) and different values of current (measured at every 100 mA). This test allows saturation effects to be analyzed.

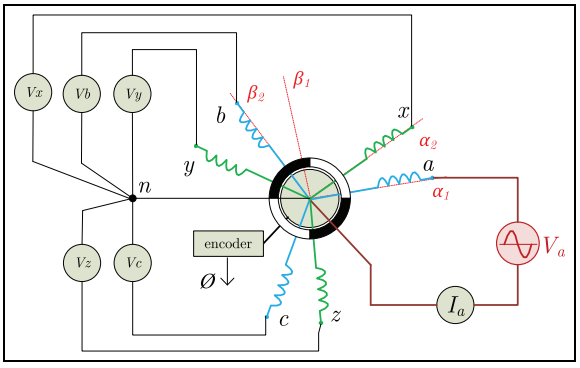

Figure 7. Connection circuit for *AC standstill method* (Dutta and Rahman, 2006).

The same tests were carried out for the symmetric machine. In Figure 12, the variations of the inductance are presented as function of the rotor position, and in Figure 13, the variations of the inductances are shown as a function of the current.

Finite-element simulation

Finite-element simulations were performed for the two modelled machines (asymmetric and symmetric). The inductances were calculated by applying equations (39) and (40) to the flux data obtained from the FEMM software.

Only the results of test $E2$ are presented, since it allows us to know the dependence of the inductance with respect to the current of the machine. Variations with respect to the rotor position are negligible, owing to the geometry of the stator and rotor.

Figures 14 and 15 show the inductances for different current values for the asymmetric and symmetric machines, respectively. It can be observed from these curves that the 2D model corresponds to the experimental results (Figures 11 and 13, respectively).

From the tests of Figures 10, 11 and 14 for the asymmetric machine ($\alpha = 30°$), substituting this angle in equation (6), we

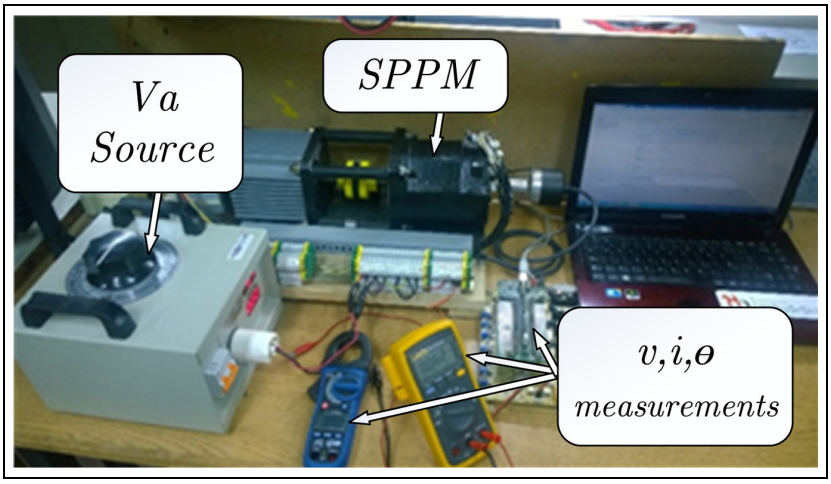

Figure 8. Experimental setup.
SPPM: six-phase polyphase machine.

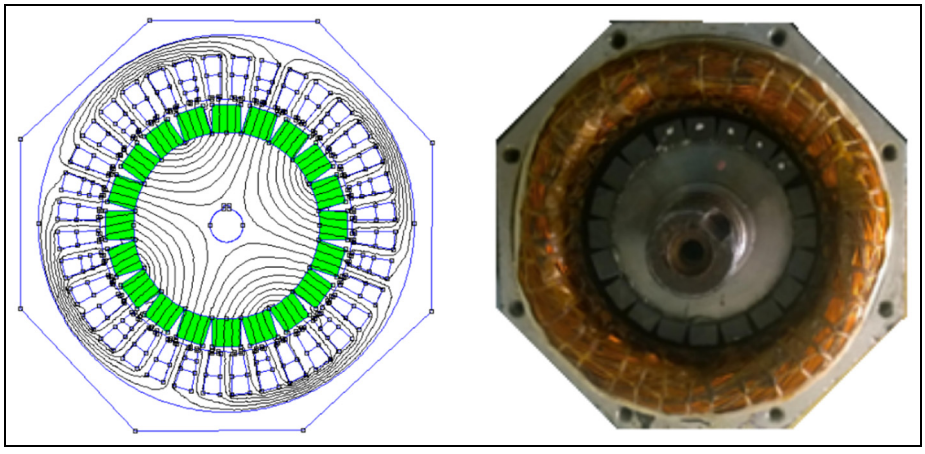

Figure 9. FE model and experimental setup of asymmetric machine.

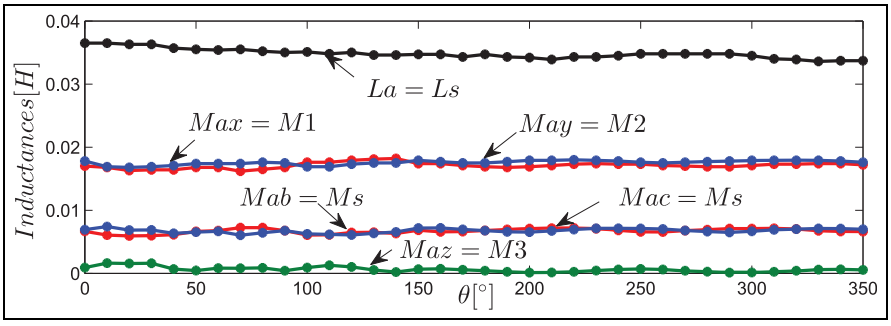

Figure 10. *E*1-asymmetric. Inductance as a function of position (experimental).

obtain that $M_s = 0.5M$, $M_1 = M_2 = (\sqrt{3}/2)M$ and $M_3 = 0$, which corresponds to the results obtained.

In the same way, from the tests of Figures 12, 13 and 15 for the symmetric machine ($\alpha = 60°$), substituting this angle

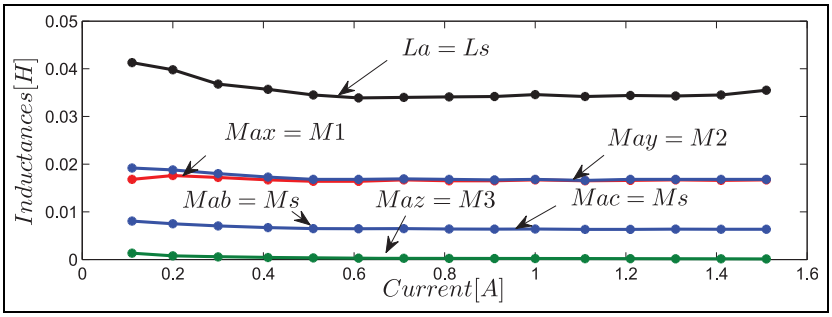

Figure 11. *E*2-asymmetric. Inductance as a function of current (experimental).

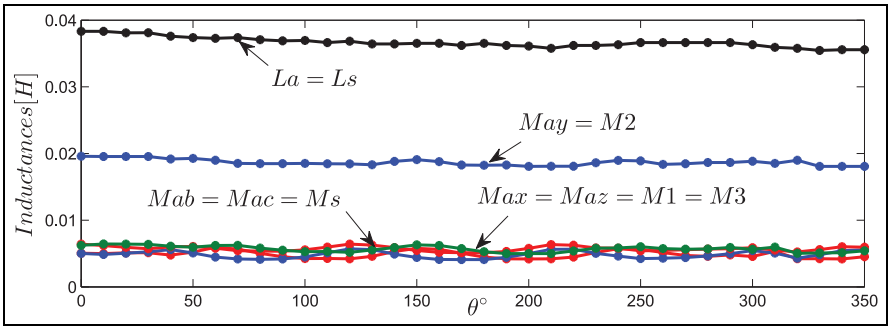

Figure 12. *E*1-symmetric. Inductance as a function of position (experimental).

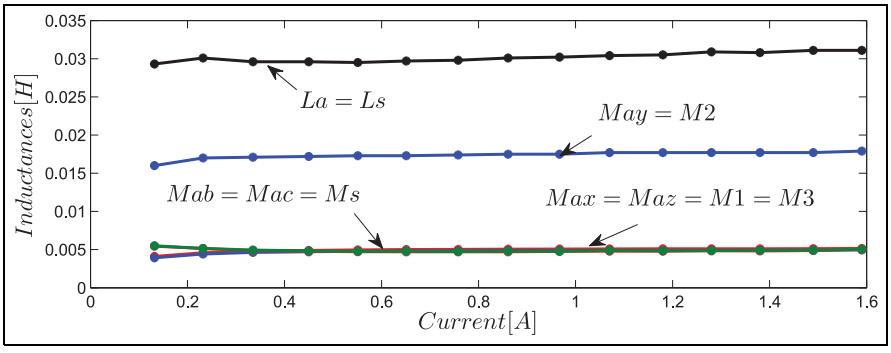

Figure 13. *E*2-symmetric. Inductance as a function of current (experimental).

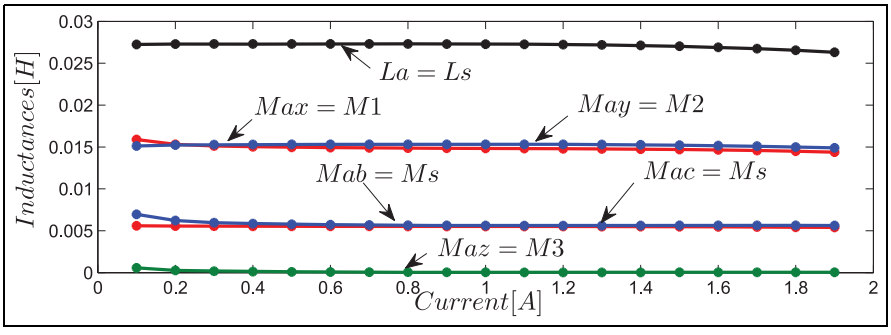

Figure 14. *E*2-asymmetric. Inductance as a function of current (finite-element simulation).

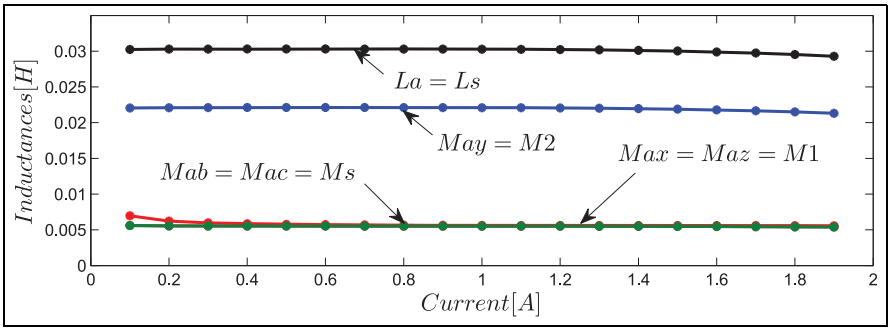

Figure 15. *E*2-symmetric. Inductance as a function of current (finite-element simulation).

Table 2. Summary of model reviews.

Model	Decoupled	Arbitrary α	Zero sequence	Reference
Vector space decomposition	Yes	Yes	Yes	Zhao and Lipo (1995)
Vector space decomposition	Yes	No	Yes	Bojoi et al. (2003)
Double three-phase	Yes	Yes	No	Nelson and Krause (1974)
Double three-phase	No	Yes	Yes	Schiferl and Ong (1983)
Double three-phase	Yes	Yes	No	Camillis et al. (2001)
Double three-phase	Yes	Yes	No	Andriollo et al. (2009)
Double three-phase	No	Yes	No	Karttunen et al. (2012)
Double three-phase	Yes	Yes	No	Kallio et al. (2013)
Double three-phase	**Yes**	**Yes**	**Yes**	**Proposed in this paper**

Table 3. Inductances, (mH).

Parameter	Asymmetric (experiment)	Asymmetric (finite-element)	Symmetric (experiment)	Symmetric (finite-element)
L_{d1}	40.8	39.6	37.8	37.9
L_{d2}	40.8	39.6	37.8	37.9
L_{d3}	75.0	74.3	68.5	70.9
L_{d4}	9.32	9.36	12.2	11.1
L_{d5}	9.32	9.36	12.2	11.1
L_{d6}	11.3	8.01	11.8	11.4

in equation (6) yields $Ms = M_1 = M_3 = 0.5M$, while $M_2 = 1M$, which validates the results obtained.

Summary of models and analysis of parameters

From the review carried out in the introduction, we conclude that there are two types of model, with different approaches; the vector space decomposition model that has been extensively studied and the double three-phase model that is treated in this work. Table 2 presents the characteristics of each of the analyzed models.

From Table 2, it is possible to observe that among the works proposing double three-phase models none other includes the zero sequence and decoupling at the same time, as the neutral is generally not connected. However, in this work, great importance is given to the connection of the neutral, since it is very useful for fault-tolerant strategies.

Six-phase machines can have two isolated neutrals, one for each three-phase system, where it is possible to use fault-tolerant strategies for four-wire systems (Catuogno et al., 2015; Meinguet et al., 2008) or a single neutral where fault-tolerant strategies can be used for seven-wire systems (Catuogno et al., 2016).

An analysis of the experimental and simulation results is presented in Table 3, were the values of inductance are calculated using equation (19). Table 3 shows inductance values of the diagonal matrix that correspond to the machine's rated current.

It can be concluded that the experimental and simulation results are very close for both machines. These procedures

allow the inductance matrix to be determined for the new model proposed in this work.

Conclusions

A novel model is proposed in this work for permanent magnet six-phase machines. In this model, the machine is considered as two three-phase systems with an arbitrary phase angle α between them and proposes an alternative to the commonly used vector space decomposition model.

The transformation **Q** allows couplings in the inductance matrix to be eliminated and can be used for any angle α. This is an important point, since it simplifies the design of the control strategies. Moreover, the transformation **Q** also includes the zero sequence, which is of relevance for fault-tolerant strategies and is the main contribution of this work.

To obtain the parameters of the model, simulations were performed using the finite-element method, which have been validated with experimental results. The experimental results were performed with a six-phase extension of a simple offline method that is used for three-phase machines.

As study cases, two traditional machines (asymmetric and symmetric) were proposed, for which the transformation matrix **Q** and its characteristic parameters were obtained.

Declaration of conflicting interests

The author(s) declared no potential conflicts of interest with respect to the research, authorship, and/or publication of this article.

Funding

The author(s) disclosed receipt of the following financial support for the research, authorship, and/or publication of this article: This work was supported by the National Scientific and Technical Research Council (CONICET) and the National University of San Luis (UNSL).

References

Andriollo M, Bettanini G, Martinelli G, et al. (2009) Analysis of double-star permanent-magnet synchronous generators by a general decoupled *d–q* model. *IEEE Transactions on Industry Applications* 45(4): 1416–1424.

Barrero F and Duran MJ (2016) Recent advances in the design, modeling, and control of multiphase machines – Part I. *IEEE Transactions on Industrial Electronics* 63(1): 449–458.

Bianchi N (2005) *Electrical Machine Analysis Using Finite Elements*. Boca Raton, FL: CRC Taylor & Frances.

Bojoi R, Lazzari M, Profumo F, et al. (2003) Digital field-oriented control for dual three-phase induction motor drives. *IEEE Transactions on Industry Applications* 39(3): 752–760.

Camillis LD, Matuonto M, Monti A, et al. (2001) Optimizing current control performance in double winding asynchronous motors in large power inverter drives. *IEEE Transactions on Power Electronics* 16(5): 676–685.

Catuogno GR, Garcia GO and Leidhold R (2015) Fault-tolerant inverter for power flow control in variable-speed four-wire permanent-magnet generators. *IEEE Transactions on Industry Electronics* 62(11): 6727–6736.

Catuogno GR, Garcia GO and Leidhold R (2016) Fault tolerant control in six-phase PMSM under four open-circuits fault conditions. In: *IECON 2016 – 42nd annual conference of the IEEE Industrial Electronics Society*, Florence, Italy, 23–26 October 2016, pp. 5754–5759. Piscataway, NJ: IEEE.

Che HS, Levi E, Jones M, et al. (2014) Current control methods for an asymmetrical six-phase induction motor drive. *IEEE Transactions on Power Electronics* 29(1): 407–417.

Dutta R and Rahman MF (2006) A comparative analysis of two test methods of measuring *d*- and *q*-axes inductances of interior permanent-magnet machine. *IEEE Transactions on Magnetics* 42(11): 3712–3718.

Kallio S, Andriollo M, Tortella A, et al. (2013) Decoupled *d-q* model of double-star interior permanent magnet synchronous machines. *IEEE Transactions on Industrial Electronics* 60(6): 2486–2494.

Karttunen J, Kallio S, Peltoniemi P, et al. (2012) Dual three-phase permanent magnet synchronous machine supplied by two independent voltage source inverters. In: *International symposium on power electronics, electrical drives, automation and motion (SPEEDAM)*, Sorrento, Italy, 20–22 June 2012, pp. 741–747. Piscataway, NJ: IEEE.

Karttunen J, Kallio S, Peltoniemi P, et al. (2014) Decoupled vector control scheme for dual three-phase permanent magnet synchronous machines. *IEEE Transactions on Industrial Electronics* 61(5): 2185–2196.

Levi E (2008) Multiphase electric machines for variable-speed applications. *IEEE Transactions on Industrial Electronics* 55(5): 1893–1909.

Levi E, Barrero F and Duran M (2016) Multiphase machines and drives – revisited. *IEEE Transactions on Industrial Electronics* 63(1): 429–432.

Meeker DC (2009) Finite Element Method Magnetics. Available at: http://www.femm.info/wiki/HomePage (accessed 25 October 2015)

Meinguet F, Semail E and Gyselinck J, (2008) Enhanced control of a PMSM supplied by a four-leg voltage source inverter using the homopolar torque. In: *18th international conference on electrical machines*, Vilamoura, Portugal, 6–9 September 2008. Piscataway, NJ: IEEE.

Munim WNWA, Duran M, Che HS, et al. (2016) A unified analysis of the fault tolerance capability in six-phase induction motor drive. *IEEE Transactions on Power Electronics* 32(10): 7824–7836.

Nelson R and Krause P (1974) Induction machine analysis for arbitrary displacement between multiple winding sets. *IEEE Transactions on Power Apparatus and Systems* PAS-93(3): 841–848.

Robbiano L (2011) Endomorphisms and diagonalization. In: Robbiano L *Linear Algebra: for Everyone*. Milan: Springer, pp:169–191.

Schiferl R and Ong C (1983) Six phase synchronous machine with AC and DC stator connections, Part I. Equivalent circuit representation and steady-state analysis. *IEEE Transactions on Power Apparatus and Systems* PAS-102(8): 2685–2693.

Underwood SJ and Husain I (2010) Online parameter estimation and adaptive control of permanent-magnet synchronous machines. *IEEE Transactions on Industrial Electronics* 57(7): 2435–2443.

Zhao Y and Lipo T (1995) Space vector PWM control of dual three-phase induction machine using vector space decomposition. *IEEE Transactions on Industry Applications* 31(5): 1100–1109.